ANTIOXIDANTS & REDOX SIGNALING
Volume 13, Number 10, 2010
© Mary Ann Liebert, Inc.
DOI: 10.1089/ars.2009.2971

ORIGINAL RESEARCH COMMUNICATION

Copper and Myeloperoxidase-Modified LDLs Activate Nrf2 through Different Pathways of ROS Production in Macrophages

Damien Calay,[1] Alexandre Rousseau,[2] Laurine Mattart,[1] Vincent Nuyens,[2] Cédric Delporte,[3] Pierre Van Antwerpen,[3] Nicole Moguilevsky,[4] Thierry Arnould,[1] Karim Zouaoui Boudjeltia,[2] and Martine Raes[1]

Abstract

Low-density lipoprotein (LDL) oxidation is a key step in atherogenesis, promoting the formation of lipid-laden macrophages. Here, we compared the effects of copper-oxidized LDLs (OxLDLs) and of the more physiologically relevant myeloperoxidase-oxidized LDLs (MoxLDLs) in murine RAW264.7 macrophages and in human peripheral blood monocyte-derived macrophages. Both oxidized LDLs, contrary to native LDLs, induced foam cell formation and an intracellular accumulation of reactive oxygen species (ROS). This oxidative stress was responsible for the activation of the NF-E2-related factor 2 (Nrf2) transcription factor, and the subsequent Nrf2-dependent overexpression of the antioxidant genes, *Gclm* and *HO-1*, as evidenced by the invalidation of Nrf2 by RNAi. MoxLDLs always induced a stronger response than OxLDLs. These differences could be partly explained by specific ROS-producing mechanisms differing between OxLDLs and MoxLDLs. Whereas both types of oxidized LDLs caused ROS production partly by NADPH oxidase, only MoxLDLs-induced ROS production was dependent on cytosolic PLA2. This study highlights that OxLDLs and MoxLDLs induce an oxidative stress, through distinct ROS-producing mechanisms, which is responsible for the differential activation of the Nrf2 pathway. These data clearly suggest that results obtained until now with copper oxidized-LDLs should be carefully reevaluated, taking into consideration physiologically more relevant oxidized LDLs. *Antioxid. Redox Signal.* 13, 000–000.

Introduction

Reactive oxygen species (ROS) are products of normal cell metabolism and play a major physiological role in intracellular signaling and regulation, such as the regulation of vascular tone, cell adhesion, or immune responses (10). However, an excessive and/or sustained increase in ROS production results in damage to cell structures (10, 40). In order to cope with an excess of ROS and the subsequent oxidative stress, humans have developed cellular mechanisms to maintain redox homeostasis. These involve antioxidant defenses such as glutathione (GSH), the major thiol antioxidant and redox buffer of the cell (11). Elevated ROS concentrations also lead to the activation of the NF-E2-related factor 2 (Nrf2) transcription factor, which is a central protein in the cellular response to oxidative stress. Once activated by ROS, Nrf2 strongly binds on DNA to the Antioxidant Response Element (46) sequence and, by this way, regulates the expression of protective genes such as the phase II drug metabolizing enzymes, as well as the regulatory subunit of glutamate-cysteine ligase (Glcm) and heme oxygenase-1 (HO-1) (16). Gclm is the rate-limiting enzyme in GSH synthesis (11). HO-1 is the rate-limiting enzyme in the degradation of heme, and induction of this enzyme causes cells to reduce their pools of heme and heme-containing proteins, eliminating potential pro-oxidants. Moreover, the by-products of this reaction—biliverdin and carbon monoxide—have antioxidant as well as anti-inflammatory properties (23, 30). Thus, it appears that Nrf2 is a key protein in the cellular response to oxidative stress and that its target genes (e.g., *Gclm* and *HO-1*) are induced for the purpose of coping with oxidative stress (19).

Despite these antioxidant defenses, when the level of ROS exceeds the antioxidant capacity of the cell, the intracellular redox homeostasis is altered and oxidative stress ensues.

[1]Laboratory of Biochemistry and Cellular Biology, University of Namur, Namur, Belgium.
[2]Experimental Medicine Laboratory (ULB 222 Unit) CHU Charleroi, ISPPC Hôpital Vésale, Montigny-Le-Tilleul, Belgium.
[3]Laboratory of Pharmaceutical Chemistry, Institute of Pharmacy, Universite Libre de Bruxelles, Brussels, Belgium.
[4]Technology Transfer Office, University of Namur, Namur, Belgium.

ARS-2009-2971-ver9-Calay_1P.3D 06/25/10 11:50pm Page 2

Oxidative stress is considered to play a pivotal role in various pathological conditions, involving cardiovascular diseases, cancer, neurological disorders, and aging (35, 40). In particular, excessive ROS production has been implicated in atherogenesis and throughout the development of this disease (35). Atherosclerosis is the major cause of heart disease and stroke, and is commonly viewed as a chronic inflammatory disease in which macrophages play a key role (18, 22). Actually, oxidative modifications of low-density lipoproteins (LDLs) contribute to the accumulation of cholesterol-loaded macrophages, termed "foam cells," that are a hallmark of the disease (18, 22, 36).

Nonetheless, although lipoprotein oxidation is well recognized to be implicated in atherogenesis (3, 36), the physiologically relevant pathways mediating these oxidative modifications have not yet been unambiguously identified. *In vitro*, the most widely studied model of LDLs oxidation involves copper ions. Indeed, free metal ions such as iron and copper have been detected in atherosclerotic lesions, and high concentrations of metal ions are potent catalysts for *in vitro* LDL oxidation. However, the concentrations of copper sulfate currently used *in vitro* to oxidize LDL (e.g., 10–20 μM) largely exceed physiological concentrations and lead to very different composition, structural, and biochemical features of the oxidized LDL (47).

That is why more recently alternative LDL oxidative pathways have been proposed involving for instance lipoxygenases (41), NAPDH oxidase (13), or myeloperoxidase (MPO) that focused our attention. MPO is certainly not the only enzyme mediating LDL oxidation *in vivo*, but there is accumulating evidence suggesting its implication in this process. Indeed, MPO, its specific by-product—3-chlorotyrosine—and MPO-oxidized LDL have been detected in human atherosclerotic lesions (8, 12, 28). Moreover, MPO strongly binds to Apo-B100 of LDL, retaining its catalytic activity. This could potentially enhance site-directed oxidation of the ApoB-100 of LDL and limit scavenging of reactive oxygen species by antioxidants (5). This enzyme may therefore represent one relevant pathway for LDL oxidation *in vivo*. Even though we are aware that MPO is not the only enzyme implicated in the *in vivo* modifications of LDL and that MoxLDL are only one kind of modified LDLs that can be found within atherosclerotic lesions, we decided to focus on LDL oxidation by MPO, which constitutes one of the more physiological mechanisms implicated in LDL oxidation (32).

The aim of this study was to highlight the differential effects of the copper-oxidized LDLs (OxLDLs) and of the physiologically more relevant myeloperoxidase-oxidized LDLs (MoxLDLs) in macrophages, using murine RAW264.7 macrophages, but also human monocyte-derived macrophages. We showed that both OxLDLs and MoxLDLs accumulate in macrophages, leading to foam cell formation, and induce an intracellular accumulation of ROS that is responsible for the activation of the Nrf2 transcription factor. Both OxLDLs and MoxLDLs also induce a ROS- and Nrf2-dependent overexpression of the antioxidant genes, *Gclm* and *HO-1*. However, MoxLDLs always induce a stronger response than OxLDLs, both in the generation of the oxidative stress and in the induction of the Nrf2 defensive pathway. We showed that this quantitative difference in the response to oxidized LDLs could be explained in part by qualitative differences in the ROS-producing mechanisms between OxLDLs and MoxLDLs.

Materials and Methods

Please see the supplemental data at www.liebertonline.com/ars for additional details.

Cell culture

The murine RAW264.7 macrophage cell line was obtained from the American Type Culture Collection (Manassas, VA) and grown in DHG-L1 medium (Dulbecco's modified Eagle's medium + high glucose (4.5 g/l) + $NaHCO_3$ (1.5 g/l)) containing 10% of heat-inactivated fetal calf serum (Gibco BRL). RAW264.7 macrophages were incubated for 1 h in DHG-L1 containing 1% of heat-inactivated serum before any treatment. Inhibitors and Trolox experiments were performed by incubating the cells with the molecules for 1 h prior to stimulation with LDLs. Cell viability was estimated using the classical LDH assay, and a maximal cytotoxicity of 30% was observed after 48 h of incubation with 200 μg/ml of oxidized LDLs. Peripheral blood mononuclear cells (PBMC) were isolated using Ficoll (Histopaque-1077, Sigma Diagnostics, St. Louis, MO) following the manufacturer's instructions. Briefly, heparinated blood was half-mixed with HBSS (Lonza, Belgium) and layered on Ficoll in a 50 ml centrifuge conical tube. After centrifugation at 400 *g* for 30 min at room temperature, the upper layer containing plasma was discarded and the interface containing the mononuclear cells (i.e., lymphocytes and monocytes) was collected. After two washes in HBSS, the mononuclear cells pellet was resuspended in RPMI 1640 + 1.5 m*M* L-glutamine (Lonza). After cell counting, mononuclear cells were diluted at a concentration of 100,000 cells/ml in RPMI 1640 + 1.5 m*M* L-glutamine, 1 m*M* sodium pyruvate, 50 μM 2-mercaptoethanol, and 1% nonessential amino acids supplemented with 10% heat-inactivated autologous serum (complete RPMI) and seeded in 6-well, 12-well, or 24-well plates. After 1 h, lymphocytes were washed away by PBS and monocytes were incubated in complete RPMI in the presence of M-CSF 20 ng/ml (R&D Systems, Abingdon, UK) for 5 days in a humidified incubator at 37°C and 5% CO_2 for macrophage differentiation (33). Medium was changed with complete RPMI containing fresh M-CSF at day 3.

LDL isolation and oxidation

Native LDLs (NatLDLs) were obtained by sequential density gradient ultracentrifugation from plasma of healthy blood donors. The concentration of NatLDL in PBS was adjusted to 1 mg/ml before incubation with 10 μM copper sulfate for 24 h at 37°C. The oxidation was stopped by the addition of 25 μM butylated hydroxytoluene and incubation on ice for 1 h. MoxLDL were generated mixing 8 μl of HCl 1 *M* (final concentration: 4 m*M*), 45 μl of recombinant human MPO (rhMPO) 92.4 U/ml (final relative activity: 4.2 U, or 2.6 U/mg LDL), a volume containing 1600 μg LDL and 40 μl of H_2O_2 50 m*M* (final concentration: 1 m*M*). The volume was adjusted to 2 ml with PBS containing 1 g/L of EDTA, at pH 6.5. Similarly, for the obtention of MoxLDL-C, 8 μl of HCl 1 *M* (final concentration: 4 m*M*), 90 μl of MPO 92.4 U/ml (final relative activity: 8.4 U, or 5.2 U/mg LDL), a volume containing 1600 μg LDL, 40 μl of H_2O_2 50 m*M* (final concentration: 1 m*M*) were mixed. The volume was adjusted to 2 ml with PBS containing 1 g/L of EDTA, at pH 4. rhMPO was provided by the Experimental Medicine Laboratory (ULB 222 Unit, CHU

◀AU1

Charleroi, Belgium). The oxidation reaction for the generation of MoxLDL and MoxLDL-C was immediately performed at 37°C for 5 and 20 min, respectively, and stopped by incubation on ice to inhibit the MPO enzymatic activity. NatLDLs, OxLDLs, MoxLDLs, and MoxLDL-C were desalted against RPMI-1640 without glutamine (Cambrex, Belgium) by using PD-10 desalting columns (GE Healthcare). LDLs were sterile filtered (0.2 μm), stored in the dark at 4°C and used within 4 days. The LDL concentration was determined by the Lowry method and used at a concentration of 200 μg/ml, concentration effectively observed in patients suffering from chronic obstructive pulmonary disease (COPD) (49) and in patients under dialysis (39).

LDL characterization

Determination of purity and alteration in negative charge in LDL preparations was carried out by an agarose gel electrophoresis. The relative electrophoretic mobilities of OxLDL, MoxLDL, and MoxLDL-C were 1.42 ± 0.17, 1.55 ± 0.14, and 1.44 ± 0.16, respectively, in comparison to NatLDL. As previously described in Zouaoui Boudjeltia *et al.* (48), the MDA-HNE content, as determined by the TBARS assay, was clearly higher in copper-oxidized LDL compared to native LDL, whereas it was similar in MoxLDL. The extent of lipid peroxidation of LDL was further estimated by a fluorescence-based method, according to Yagi *et al.* (42) (see supplemental data; Fig. 8A.). Compared to NatLDLs, OxLDLs showed an increased lipid peroxidation while it was only slightly increased in MoxLDLs. The lipid peroxidation content of MoxLDLs-C was intermediate as it was clearly higher than in MoxLDLs but was much more moderate compared to OxLDLs.

Statistics

SigmaStat software (Jandle Scientific, Germany) was used for the analysis. Data are presented as means $\pm$ SEM and were evaluated by one-way ANOVA, using the Holm-Sidak method.

Results

Macrophages incubated with MoxLDLs accumulate more lipid droplets and display a very distinct morphology compared to OxLDLs-incubated macrophages

The ability of the murine RAW264.7 macrophages to accumulate modified LDLs and consequently to differentiate into foam cells was first assessed. RAW264.7 macrophages were therefore treated with native or oxidized LDLs for 48 h before lipid staining by Oil Red O (Sigma, St. Louis, MO) or Bodipy® (Invitrogen, Carlsbad, CA) Fig. 1A, top and middle panels, respectively). Both stainings clearly show that macrophages internalize NatLDLs in a regulated manner as only a small number of intracellular lipid droplets is observed. Indeed, native LDLs are recognized by the LDL receptor (LDL-R) that is downregulated by the intracellular cholesterol content through a signaling pathway implicating SREBP (45). Thus, the internalization of native LDLs is tightly controlled and never leads to an excessive accumulation of intracellular lipid droplets and subsequent foam cell formation. On the opposite, large amounts of lipid droplets are observed throughout the cytoplasm of both OxLDLs- and MoxLDLs-incubated macrophages (Fig. 1A). A quantification of the Oil Red O staining after 30 min to 48 h (Figure 1B) confirmed these observations, with OxLDLs and MoxLDLs, respectively, causing an intracellular 2.9 ± 0.26 and 4.1 ± 0.37 fold accumulation of lipids after 48 h compared to control cells. A significant accumulation of lipid droplets was observed after 48 h of incubation with NatLDLs, probably due to some oxidation of the NatLDL in the contact of the cells for long periods of time. However, a significant accumulation of lipid droplets was already observed after 24 h and 2 h of incubation with OxLDLs or MoxLDLs, respectively. Moreover, the MoxLDLs-induced accumulation of lipids was significantly higher than the one caused by OxLDLs. In addition, whereas RAW264.7 macrophages incubated with OxLDLs appeared very rounded, a more typical spread morphology of macrophages, with long cytoplasmic extensions, was observed in the presence of MoxLDLs (Fig. 1A, top panel). The accumulation of intracellular lipid droplets was confirmed in human M-CSF differentiated macrophages prepared from PBMC, although more difficult to visualize, due to larger amounts of lipids in control cells and in NatLDLs-treated cells (Fig. 1A, bottom panel). However, the quantification of the Oil Red O staining showed that the incubation with both oxidized LDL induced an accumulation of intracellular lipid droplets, but to a lesser extent than in RAW264.7 macrophages (Fig. 1C). Moreover, it seems that the internalization was more important in MoxLDLs-treated macrophages than in OxLDLs-incubated cells, as observed for the murine RAW264.7 cells.

Oxidized LDLs induce an intracellular oxidative stress in RAW264.7 and in human PBMC-derived macrophages

Oxidized LDLs are claimed to largely contribute to the oxidative context of atherosclerosis (36). To directly assess this oxidative stress, RAW264.7 and PBMC-derived macrophages were incubated with native or oxidized LDLs (200 μg/ml) and the intracellular accumulation of ROS was monitored (Figs. 2A and 2B, respectively). In RAW264.7 macrophages, where NatLDLs had no effect, an accumulation of ROS was observed in the presence of oxidized LDLs. However, the oxidative stress produced by the MoxLDLs was more intense than the one caused by OxLDLs (Fig. 2A). Trolox, an antioxidant and hydrophilic vitamin E analogue, totally abolished the oxidized LDL-induced ROS accumulation (Fig. 2A). This accumulation of ROS was also observed in PBMC-macrophages incubated with OxLDLs or MoxLDLs, whereas in incubations with NatLDLs, a decrease in oxidative stress was observed (Fig. 2B). Moreover, a clear difference was observed between OxLDLs and MoxLDLs-induced ROS accumulation as OxLDLs only induced a slight increase in ROS production, whereas it was more intense for MoxLDLs (Fig. 2B).

Oxidized LDLs activate the transcription factor Nrf2 in a ROS-dependent manner

As Nrf2 is a well-known ROS-activated transcription factor (16, 19), its activation state in RAW264.7 macrophages after incubation with native or oxidized LDLs was assessed using a reporter plasmid. The stimulation of macrophages with oxidized LDLs induced the activation of Nrf2 (Fig. 3),whereas, similarly as for the ROS production, the incubation of macrophages with NatLDLs did not. Moreover, MoxLDLs

ARS-2009-2971-ver9-Calay_1P.3D 06/25/10 11:50pm Page 4

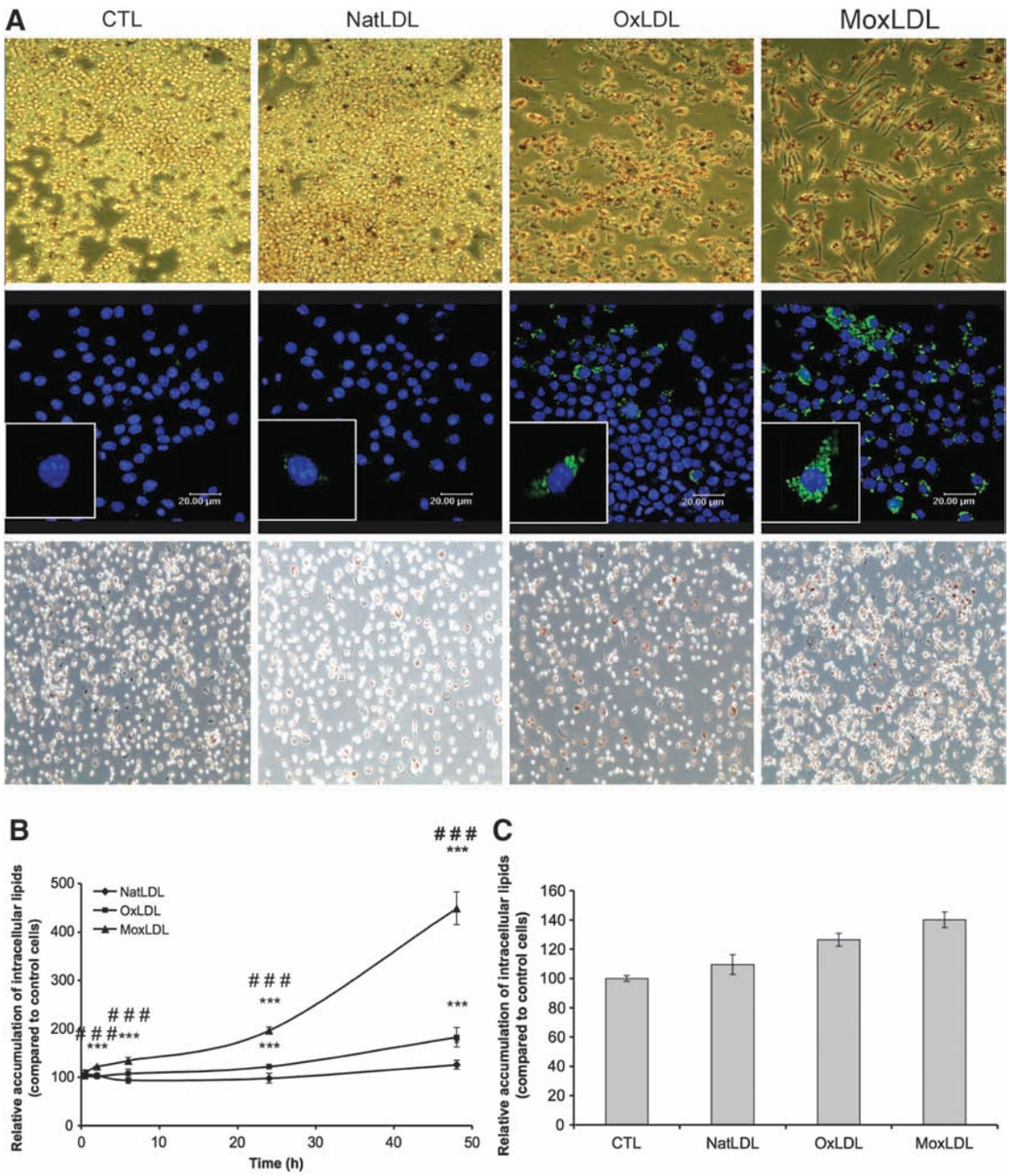

FIG. 1. Differential lipid accumulation in macrophages incubated with OxLDLs or MoxLDLs. RAW264.7 cells (**A**, top and middle panels, **B**) and human PBMC-derived macrophages (**A**, bottom panel, and **C**) were incubated for 48 h with native or oxidized LDLs (200 μg/ml), stained with Oil Red O (**A**, top and bottom panels) or Bodipy (**A**, middle panel) and visualized with an optical (objective 20X) or a confocal microscope, respectively. (**B**) The absorbance of Oil Red O staining was normalized by the quantity of cells. Results represent the mean of four replicates ± SEM. N.S. = nonsignificant, $^{***}p < 0.001$ MoxLDL vs. control; $^{\S\S\S}p < 0.001$ OxLDL vs. control; $^{\#\#\#}p < 0.001$ OxLDL vs. MoxLDL.

triggered a significantly stronger activation of Nrf2 than OxLDLs (Fig. 3). The regular addition of Trolox significantly decreased the oxidized LDLs-induced activation of Nrf2 (Fig. 3), which suggests a prevalent role of ROS in this activation.

Oxidized LDLs induce the overexpression of the antioxidant genes, Gclm and HO-1

Following oxidative stress, cells activate a global transcriptional response, notably through Nrf2, in order to counteract the accumulation of ROS. Among the genes involved in this response, *Gclm* and *HO-1* play a crucial role in the generation of antioxidants such as glutathione and bilirubin. The relative abundance of the mRNA for these two genes was evaluated after incubation of the RAW264.7 macrophages with 200 μg/ml of native or oxidized LDLs (Figs. 4A and 4B). NatLDLs were unable to induce an overexpression neither of *Gclm* nor *HO-1*, in comparison to control cells. However, the mRNA abundance of both genes was increased after incubation with OxLDLs or MoxLDLs (Figs. 4A and 4B). ◀F4

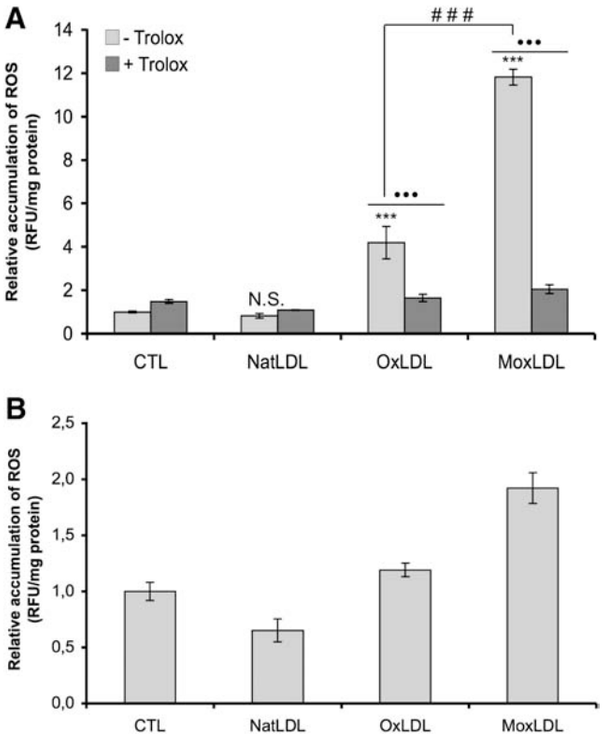

FIG. 2. Oxidized LDLs induce an intracellular accumulation of ROS that can be abolished by Trolox. Macrophages loaded with the H_2DCF-DA probe were stimulated with native or oxidized LDLs (200 μg/ml) in the presence or absence of Trolox 500 μM for 6 h. The fluorescence of oxidized DCF was normalized by the protein quantity and compared to control cells arbitrarily set to 1. The graph **A** is the mean of three replicates ± SEM and is representative of two independent experiments. N.S. = nonsignificant, $^{***}p < 0.001$ vs. control; $^{\#\#\#}p < 0.001$ OxLDL vs. MoxLDL; $^{\bullet\bullet\bullet}p < 0.001$ absence vs. presence of Trolox.

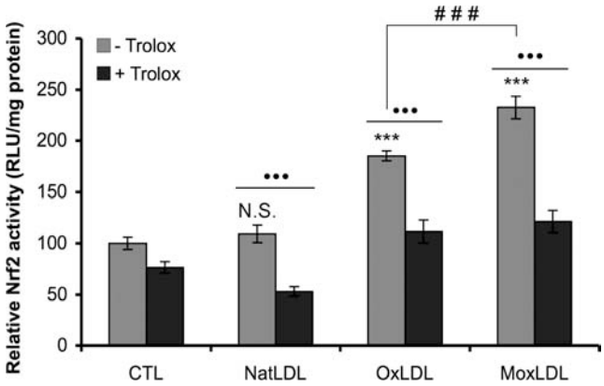

FIG. 3. Oxidized LDLs, but not native LDLs, induce the activation of Nrf2. After the transfection with the ARE-luc reporter plasmid, the macrophages were incubated with native or oxidized LDLs (200 μg/ml) in the presence or absence of Trolox (500 μM). Results were compared to control cells arbitrarily set to 1 and are given as the mean of six replicates ± SEM. N.S. = nonsignificant, $^{***}p < 0.001$ vs. control; $^{\#\#\#}p < 0.001$ OxLDL vs. MoxLDL; $^{\bullet\bullet\bullet}p < 0.001$ absence vs. presence of Trolox.

For *Gclm*, a peak of overexpression was observed after 6 h of incubation with OxLDLs or MoxLDLs, but again differences between the OxLDLs-induced and MoxLDLs-induced overexpression were remarkable throughout the kinetics (Fig. 4A). Regarding *HO-1*, the maximal overexpression was detected after 4 h of incubation with MoxLDLs, whereas the peak of expression was more attenuated and observed after 6 h of incubation with OxLDLs. Moreover, a second wave of overexpression was observed after 12 h of incubation of the macrophages with MoxLDLs, which was not seen with OxLDLs (Fig. 4B.). The overexpression of *HO-1* was also observed in human PBMC-derived macrophages incubated with 200 μg/ml of oxidized LDL for 6 h (Fig. 4C). This overexpression was not observed when the cells were incubated with NatLDLs. Moreover, MoxLDLs induced a stronger overexpression of *HO-1* than OxLDLs. In RAW264.7 macrophages, the overexpression of *HO-1* and *Gclm* after oxidized LDLs treatment was confirmed at the protein level (Fig. 4D). Whatever the time of incubation (from 2 to 24 h), NatLDLs did never induce an increased abundance neither of Gclm nor HO-1, in comparison to control cells (Fig. 4D). However, the abundance of Gclm was increased and maximal after 12 h of incubation with OxLDLs or MoxLDLs, and much more pronounced in the presence of MoxLDLs (Fig. 4D). While MoxLDLs induced a peak of abundance for HO-1 between 8 and 12 h of incubation, this peak was more attenuated and clearly observed after 8 h of incubation with OxLDLs. Moreover, contrary to MoxLDLs, the OxLDLs-induced HO-1 overexpression returned to basal levels after 24 h (Figure 4D). These observations were confirmed by immuno-ytochemistry using confocal microscopy (Fig. 4E).

Oxidized LDLs-induced overexpression of Gclm and HO-1 is partly mediated by ROS

Gclm and *HO-1* are induced by numerous stimuli, which have in common that they produce an oxidative stress through ROS production (2, 11). Therefore, in order to assess the role of the oxidized LDL-induced ROS production in the overexpression of these genes, macrophages were incubated in the presence of Trolox, shown to abolish the ROS production (Fig. 2A). As shown respectively in Figures 5A and 5B, the oxidized LDL-induced overexpression of *Gclm* and *HO-1* was significantly reduced by the addition of Trolox. For *Gclm*, we observed a 2.9- and 3.2-fold reduction in the abundance of mRNA for OxLDLs and MoxLDLs, respectively; for *HO-1*, we obtained a 2.1- and 2.5-fold reduction, respectively, for OxLDLs and MoxLDLs. While the addition of Trolox completely abolished the accumulation of ROS induced by oxidized LDLs (Fig. 2), it was unable to reduce the expression of *Gclm* and *HO-1* to their basal levels, supporting the hypothesis that other pathways, independent of ROS, are involved in the oxidized LDLs-induced overexpression of *Gclm* and in particular of *HO-1*.

Nrf2 is the major transcription factor involved in the oxidized LDLs-induced overexpression of Gclm and HO-1

To assess the specific contribution of Nrf2 in the LDLs-induced overexpression of *Gclm* and *HO-1*, the RNA

ARS-2009-2971-ver9-Calay_1P.3D 06/25/10 11:53pm Page 6

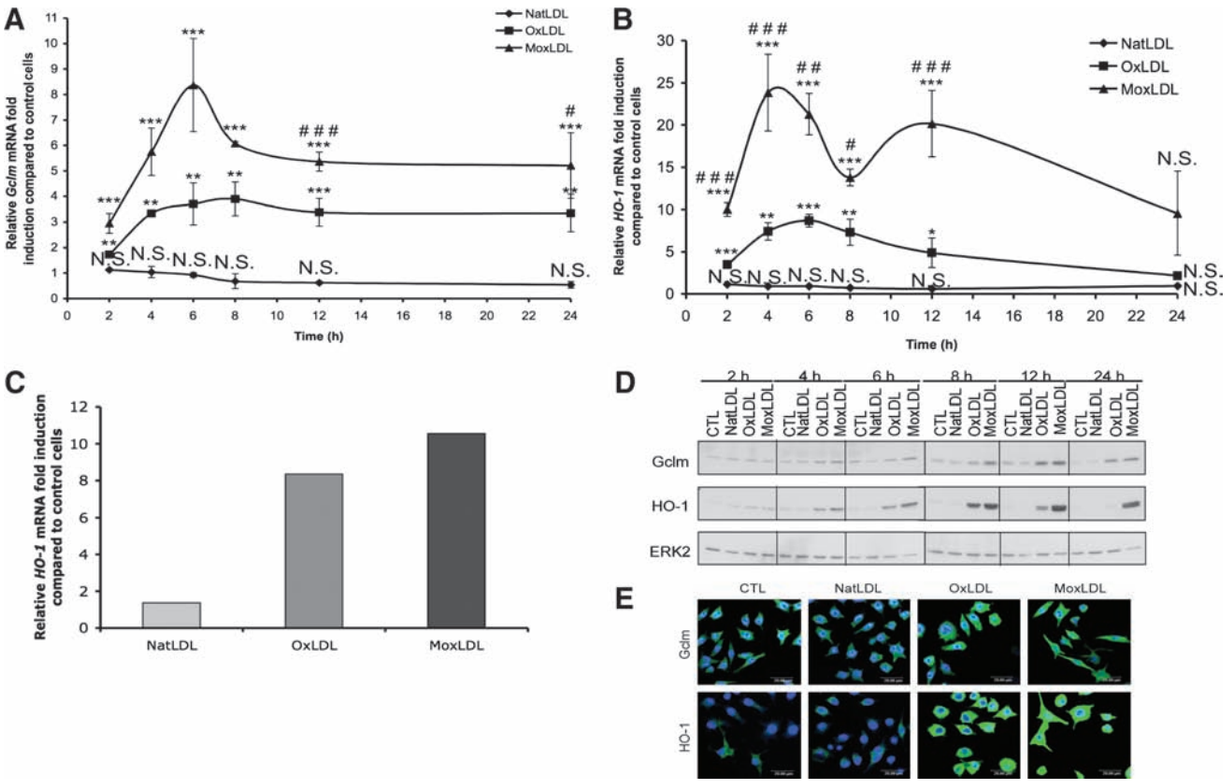

FIG. 4. ***Gclm* and *HO-1* are induced by oxidized LDLs.** RAW264.7 and PBMC-derived macrophages were incubated with 200 μg/ml of native or oxidized LDLs for indicated times and 6 h, respectively (**A–C**). The relative abundance of *Gclm* (**A**) and *HO-1* (**B** and **C**) mRNA was evaluated by real-time RT-PCR and compared to control cells arbitrarily set to 1. TBP and 18S were used as housekeeping gene for RAW264.7 and PBMC-derived macrophages, respectively. Results are given as the mean of four replicates ± SEM. (**D**) Cell lysates were subjected to SDS-PAGE and immunoblotting, and the relative protein abundance of Gclm and HO-1 was revealed by chemiluminescence. ERK2 was used as loading control. (**E**) RAW264.7 macrophages were treated with native or oxidized LDLs (200 μg/ml) for 6 h before Gclm or HO-1 fluorescent immunostaining and visualization by confocal microscopy, with the nuclei in *blue* (Topro) and the proteins in *green* (Alexa 488) (objective 63X). The experiments on RAW264.7 macrophages are representative of two independent replicates. N.S. = non-significant, $^{*}p < 0.05$, $^{**}p < 0.01$, $^{***}p < 0.001$ vs. control; $^{\#}p < 0.05$, $^{\#\#}p < 0.01$, $^{\#\#\#}p < 0.001$ OxLDL vs. MoxLDL.

interference strategy was applied. The invalidation of Nrf2 led to a strong reduction of the MoxLDLs-induced overexpression of *Gclm* and *HO-1* (Figs. 6A and 6B). However, whereas this invalidation totally abolished the overexpression of *Gclm*, for *HO-1*, we still observed an overexpression compared to control cells, suggesting that other transcription factors activated by oxidized LDLs could intervene in its overexpression. The oxidized-LDLs induced overexpression of Gclm (data not shown) and HO-1 (Fig. 6C) at the protein level was also clearly reduced by the invalidation of Nrf2, whereas transfection of RAW264.7 macrophages with nontargeting siRNA had no effect.

F6 ▶

NADPH oxidase plays a role in the ROS production induced by both oxidized LDLs, but cytosolic PLA2 are involved only in MoxLDLs-treated cells

Searching to elucidate some of the molecular mechanisms responsible for the oxidized LDLs-induced ROS production, we showed that the use of diphenylene iodonium (DPI), which inhibits NADPH oxidase, significantly reduced both OxLDLs- and MoxLDLs-induced ROS accumulation (Fig. 7A). However, DPI was unable to completely abolish the ROS production even when used at 100 μM (Fig. 7A), supporting the fact that other ROS generating enzymes than NADPH oxidase are implicated in oxidized LDLs-induced ROS accumulation.

F7 ▶

Several studies highlight that oxidized LDLs activate the Ca^{2+}-dependent and Ca^{2+}-independent cytosolic phospholipase A2 (cPLA2 and iPLA2, respectively), which results in the specific release of arachidonic acid (AA) (1, 21), and the subsequent activation of NADPH oxidase (34), although this pathway of ROS production by AA is not exclusive (17). Hence, the effect of methyl arachidonyl fluorophosphonate (MAFP), an inhibitor of both Ca^{2+}-dependent and Ca^{2+}-independent cytosolic PLA2, on the oxidized LDLs-induced ROS production was evaluated. As shown in Figure 7B, while MAFP did not decrease the OxLDLs-induced generation of ROS, it significantly reduced the MoxLDLs-generated ROS accumulation by 43%. When exogenous AA was added together with MAFP, ROS production not only was recovered but was even higher than with the oxidized LDLs (Fig. 7B). The effect of MAFP on the intracellular accumulation of lipids was also investigated. As shown in Figure 7C, no difference

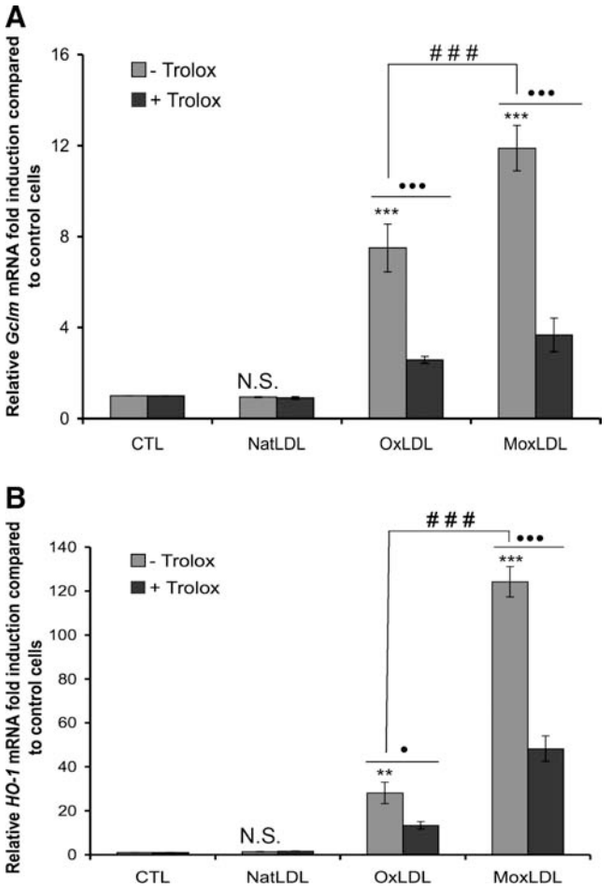

FIG. 5. Trolox reduces the oxidized LDLs-induced overexpression of *Gclm* and *HO-1*. The cells were stimulated with native or oxidized LDLs (200 μg/ml) for 6 h in the presence or absence of Trolox 500 μM. The relative abundance of *Gclm* and *HO-1* mRNA was evaluated by real-time RT-PCR and results are expressed as in Figure 4 and given as the mean of four replicates ± SEM. N.S. = nonsignificant, $^{**}p < 0.01$, $^{***}p < 0.001$ vs. control; $^{\#\#\#}p < 0.001$ OxLDL vs. MoxLDL; $^{\bullet}p < 0.05$, $^{\bullet\bullet\bullet}p < 0.001$ absence vs. presence of Trolox.

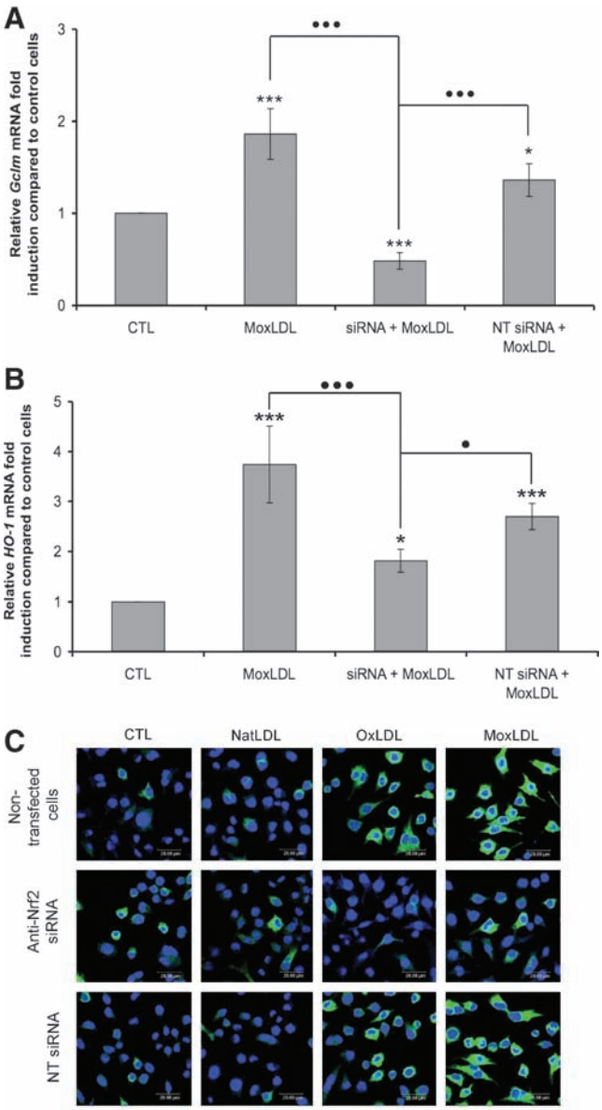

FIG. 6. Oxidized LDLs-induced *Gclm* and *HO-1* overexpression is essentially mediated by Nrf2. RAW264.7 cells were transfected with anti-Nrf2 siRNA or nontargeting (NT) siRNA. After stimulation with 200 μg/ml of MoxLDLs for 2 h, the relative abundance of *Gclm* (**A**) and *HO-1* (**B**) mRNA was evaluated by real-time RT-PCR. Results are expressed as previously described and given as the mean of three replicates ± SEM. (**C**) RAW264.7 cells transfected with anti-Nrf2 siRNA or nontargeting (NT) siRNA were incubated with 200 μg/ml of native or oxidized LDLs for 6 h. Gclm and HO-1 were visualized by confocal microscopy, as described in Figure 4. $^{*}p < 0.05$, $^{***}p < 0.001$ vs. control; $^{\bullet}p < 0.05$ siRNA + MoxLDL vs. MoxLDL or NT siRNA + MoxLDL, $^{\bullet\bullet\bullet}p < 0.001$ siRNA + MoxLDL vs. MoxLDL or NT siRNA + MoxLDL.

was observed between macrophages incubated in the presence or in the absence of MAFP for 48 h. Therefore, it seems that PLA2 (at least cPLA2 and iPLA2) is not implicated in foam cell formation of macrophages incubated with OxLDLs or MoxLDLs. In conclusion, whereas NADPH oxidase is in part implicated in both OxLDLs- and MoxLDLs-induced ROS production, only the MoxLDLs-induced ROS generation seems to implicate cytosolic PLA2 and the subsequent AA release. Moreover, despite its role in MoxLDLs-induced ROS production, cytosolic PLA2 are not implicated in the accumulation of intracellular lipid droplets in macrophages incubated with OxLDLs or MoxLDLs.

LDLs oxidized at both the lipid and protein moieties by MPO behave betwixt Ox- and MoxLDLs

Based on the results obtained in Figure 7, and on the fact that MoxLDLs, contrary to OxLDLs, are only slightly modified at the lipid level (Fig. 8A) (48), we hypothesized that the fatty acids that are not modified and in particular arachidonic acid (AA), can be released from the MoxLDLs by cytosolic PLA2 and subsequently trigger ROS production. To support this hypothesis, we generated MoxLDLs oxidized at the lipid moiety (28), named MoxLDLs-C (see Materials and Methods;

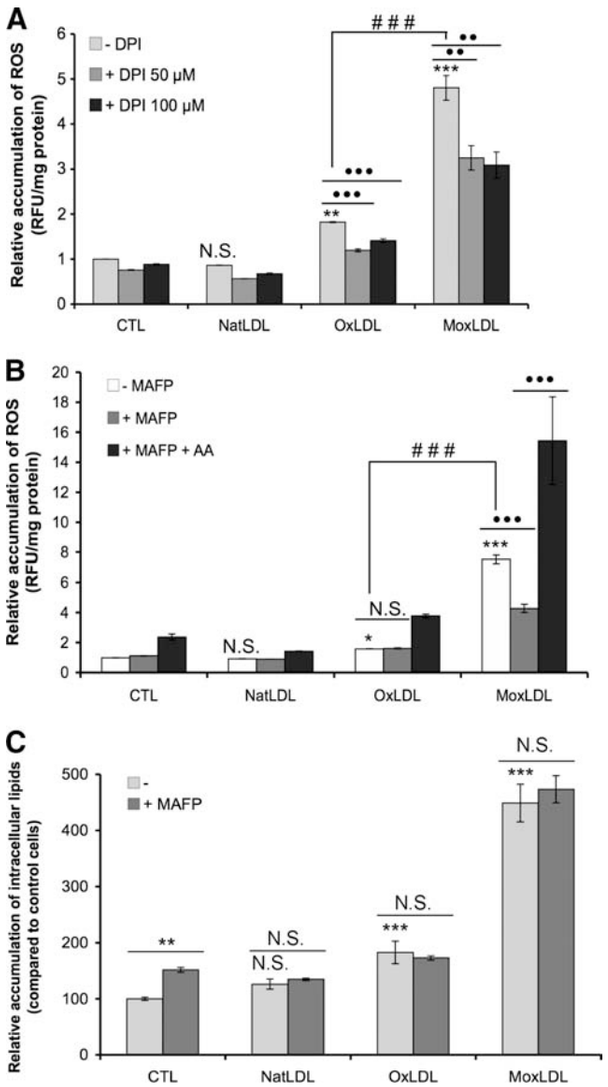

FIG. 7. Effects of DPI and MAFP on ROS production induced by oxidized LDLs. RAW264.7 macrophages loaded with the H_2DCF-DA dye were stimulated with native or oxidized LDLs (200 μg/ml), and/or AA (20 μM) in the presence of DPI (50 μM or 100 μM) (**A**) or MAFP (50 μM, **B**). After 30 min, the fluorescence of oxidized DCF was measured and expressed as described in Figure 1. Results are given as the mean of three replicates ± SEM. N.S. = nonsignificant, $^{*}p < 0.05$, $^{**}p < 0.01$, $^{***}p < 0.001$ vs. control; $^{\#\#\#}p < 0.001$ OxLDL vs MoxLDL; $\bullet\bullet p < 0.01$ absence vs. presence of the inhibitor, $\bullet\bullet\bullet p < 0.001$ absence vs. presence of the inhibitor or MAFP vs MAFP + AA.

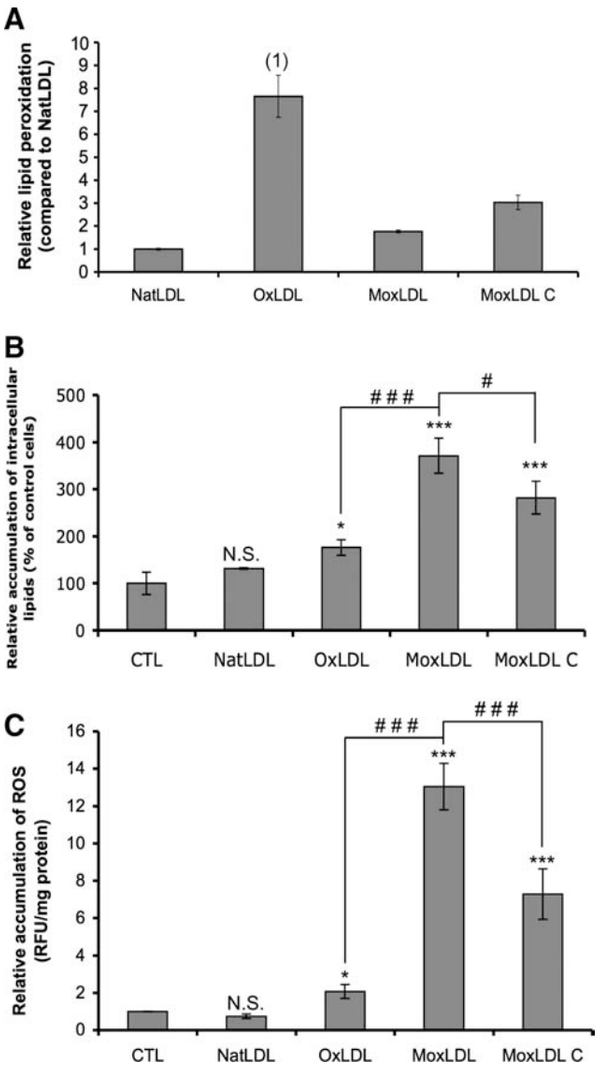

FIG. 8. Effects of the lipid peroxidation extent of LDLs on foam cell formation and on intracellular ROS accumulation. Lipid peroxidation of native and oxidized LDLs was evaluated by a fluorescence-based method as described in the Materials and Methods. The extent of lipid peroxidation was expressed in comparison to NatLDLs arbitrarily set to 1 (**A**). RAW264.7 macrophages were incubated for 48 h with native or oxidized LDLs (200 μg/ml), stained with Oil Red O, and the absorbance of the staining was normalized by the quantity of cells (**B**). Cells loaded with the H_2DCF-DA dye were stimulated with native or oxidized LDLs (200 μg/ml). After 30 min, the fluorescence of oxidized DCF was measured and expressed as described in Figure 1 (**C**). Results are given as the mean of three replicates ± SEM. N.S. = nonsignificant, $^{*}p < 0.05$, $^{***}p < 0.001$ vs. control; $^{\#}p < 0.05$, $^{\#\#\#}p < 0.001$ OxLDL or MoxLDL-C vs. MoxLDL; (1) based on the results of Zouaoui Boudjeltia *et al.* (48).

Fig. 8A). To confirm the lipid modification of MoxLDLs-C, the extent of lipid peroxidation in NatLDLs, MoxLDLs, and MoxLDLs-C was determined by a fluorescence-based method, according to Yagi *et al.* (42) (Fig. 8A). Zouaoui Boudjeltia *et al.* (48) already showed that lipid peroxidation in OxLDLs was much more intense in comparison to NatLDLs (Fig. 8A). In striking contrast, lipid peroxidation was only slightly increased in MoxLDLs, supporting the statement that MoxLDLs mainly used in this work are almost not modified at the lipid level. The analysis of MoxLDLs-C showed elevated levels of lipid peroxidation in comparison to MoxLDLs, but this increase was lower than in OxLDLs (Fig. 8A). Therefore, lipid oxidation of MoxLDLs-C is intermediate between OxLDLs

ARS-2009-2971-ver9-Calay_1P.3D 06/25/10 11:56pm Page 9

and MoxLDLs. In the same way as the incubation with OxLDLs or MoxLDLs, the treatment of RAW264.7 macrophages with MoxLDLs-C for 48 h also induced a significant accumulation of intracellular lipid droplets (Fig. 8B). Furthermore, we showed that the MoxLDLs-C-induced ROS production after 30 min was lower when compared to MoxLDLs, but higher compared to OxLDLs (Fig. 8C). Interestingly, this result suggests that ROS production is inversely related to the extent of lipid peroxidation observed in the different types of modified LDL (Fig. 8A).

Discussion

The oxidative modifications of LDLs contribute to the pathogenesis of atherosclerosis, and the presence of cholesterol-loaded macrophages is an important feature throughout the development of the lesion. However, *in vivo* neither the mechanisms nor the site of LDLs oxidation are totally elucidated. Oxidative modifications of LDLs are often produced *in vitro* by the use of copper ions. However, in 1996, Berliner and Heinecke already provided data questioning the role of copper in *in vivo* LDL oxidation (3). This was sustained afterwards by numerous data and studies. First of all, low concentrations of albumin, the most abundant protein in plasma, inhibit metal ion-dependent LDL oxidation, and this protein also avidly binds free copper (37). Indeed, there is no convincing evidence that either free iron or copper do exist in plasma, and extracellular free metal ions are, therefore, unlikely to be present in normal arterial tissue. Metal ions might become available under pathologic conditions, however, perhaps as a result of dying cells accumulating in advanced atherosclerotic lesions. On the other hand, even if copper could have a potential role in LDL oxidation *in vivo*, the concentrations of copper sulfate currently used *in vitro* to oxidize LDL (e.g., 10 to 20 μM), largely exceed physiological concentrations (47). Ziouzenkova and collaborators notably underlined that LDL oxidized with copper sulfate used at the concentration of 0.03 μM, which is in the range of physiological concentrations, display major differences in composition compared to LDL oxidized using copper sulfate at 10 μM (47). Concomitantly with numerous other studies, these authors emphasized that it is uncertain if this *in vitro* model reflects any aspects of LDL oxidative modification *in vivo*. In 2003, this was also corroborated by Zarev and collaborators who highlighted that the use of low concentrations of copper, far below the saturation of the LDL binding sites and capable to initiate low LDL oxidation rates, could be more relevant regarding *in vivo* LDL oxidation (46). They also showed that different concentrations of copper not only lead to significant differences in LDL oxidation kinetics, but also to different forms of oxidized LDL with specific physicochemical and probably biological features (46).

Alternatively, oxidizing enzymes present in pro-inflammatory conditions have been proposed to play a role in the *in vivo* oxidation of LDL, such as lipoxygenases (in particular 15-lipoxygenase) (41), NADPH oxidase (13), and MPO, that was privileged in this work. MPO is found as a catalytically active enzyme within atherosclerotic lesions, as evidenced by the presence of immuno-detected MPO, its specific products, as well as MPO-modified LDLs, suggesting a role for this enzyme in the *in vivo* modifications of LDLs (8, 12, 28). Moreover, in atherosclerotic lesions, MPO colocalizes with macrophage-derived foam cells (*8*) and is able to strongly bind to Apo-B100 of LDL (5). Finally, using mass spectrometry, Leeuwenburgh *et al.* detected a 100-fold selective increase in o,o′-dityrosine levels in LDL isolated from human atherosclerotic lesions compared to circulating LDLs. Although *in vitro* incubation of LDL with copper increased both o-tyrosine and m-tyrosine, little change in the level of o,o′-dityrosine was observed. In contrast, o,o′-dityrosine was selectively produced in LDL oxidized with tyrosyl radical generated by myeloperoxidase (20). Therefore, the detection of a selective increase in o,o′-dityrosine levels with limited changes in either o-tyrosine or m-tyrosine in LDL isolated from human vascular lesions, is consistent with the hypothesis that oxidative damage in human atherosclerosis is mediated in part by tyrosyl radical generated by myeloperoxidase. MPO is therefore considered as one of the potential enzymes implicated in LDL oxidation *in vivo (32)*.

However, in striking contrast with a deleterious role for MPO in atherogenesis through its implication in LDL oxidation, MPO-deficient mice developed 50% larger atherosclerotic lesions than WT mice (4). Nonetheless, MPO levels are 5-fold to 10-fold higher in humans than in mice and MPO regulation may also differ significantly. Moreover, in contrast to human atherosclerotic lesions that readily stain for MPO (8) and show clear evidence of 3-chlorotyrosine (12), only small amounts of MPO are found within murine atherosclerotic lesions and the 3-chlorotyrosine levels observed in the mouse are barely above the limit of detection (4), suggesting limited catalytically active MPO in the artery wall in mice. Therefore, although mouse models have provided important insights into the pathogenesis of atherosclerosis, the limited levels of MPO and 3-chlorotyrosine observed in mouse atheroma might at first glance suggest that the murine model has limited relevance for studies of MPO in atherosclerosis.

In order to better evaluate the role of human MPO (h-MPO) in atherogenesis, McMillen *et al.* generated transgenic mice that expressed h-MPO exclusively in macrophages (27). This cell-specific expression of h-MPO increased the average size of the atherosclerotic lesions by 2.3-fold compared to mice transplanted with WT bone marrow. The larger atherosclerotic lesions observed in MPO-deficient mice and in transgenic mice expressing h-MPO in macrophages strongly suggest that MPO from neutrophils and monocytes play a role in atherogenesis that is distinct from that of macrophage-associated MPO in the artery wall. This supports the hypothesis that macrophage-specific expression of MPO is atherogenic and raises the possibility that lipoprotein oxidation via MPO is an important mechanism.

Copper and myeloperoxidase induce some distinct biochemical alterations of LDLs (44). Actually, the oxidation of LDLs with copper ions causes important modifications of both the lipid and protein moieties of the LDLs (46). On the other hand, MoxLDLs used in this work are predominantly modified only in their protein moiety, with limited modifications of the lipids (24, 48). Moreover, the concentrations of MoxLDLs used (200 $\mu g/ml$) correspond to pathophysiological concentrations indeed observed in patients suffering from COPD (49) or undergoing dialysis (39) and prone to cardiovascular disease.

Interestingly, the signal transduction pathways activated by OxLDLs are relatively well-known and the active compounds identified up to now are generally lipids (26). Much

ARS-2009-2971-ver9-Calay_1P.3D 06/25/10 11:56pm Page 10

less information is available about MoxLDLs and although numerous studies have characterized the cellular responses either to OxLDLs or, to a lesser extent, to MoxLDLs, comparative studies are much more difficult to find. For these reasons, in this study, the differential effects of OxLDLs and MoxLDLs were compared in RAW264.7 macrophages and the results were partly validated in human PBMC-derived macrophages.

First of all, we showed that macrophages incubated with MoxLDLs accumulate more intracellular lipid droplets than when incubated with OxLDLs. Given the differential modifications of ApoB-100 by copper and the MPO–H_2O_2–Cl^- system (44), a differential affinity for or a differential recognition by the diverse scavenger receptors could be a possible explanation to interpret this distinction. Although the scavenger receptors for OxLDLs are well described and comprise predominantly SR-A and CD36, those for MoxLDLs are not yet unambiguously identified. Nevertheless, *in vitro* studies on THP-1 macrophages have shown that class B scavenger receptors, namely CD36 and SR-BI, play a role in the internalization of MoxLDLs (25). The specific scavenger receptors implicated in the internalization of OxLDLs and more particularly of MoxLDLs should certainly deserve more attention. On the other hand, the incubation of macrophages with OxLDLs or MoxLDLs also differentially affects their morphology. RAW264.7 macrophages incubated with MoxLDLs display a characteristic spreaded morphology while they remain rounded in the presence of OxLDLs. Although OxLDLs could affect cytoskeletal components, such as actin or vimentin (9, 31), the effect of MoxLDLs on these proteins is still not known, and could explain the observed differential morphology.

Second, in view of the biochemical differences between OxLDLs and MoxLDLs, it is not surprising to observe differences between OxLDLs and MoxLDLs in the activation of Nrf2 and the induction of *Gclm* and *HO-1*, with a stronger response towards MoxLDLs. The protective and stress-induced Nrf2 pathway is functionally critical and tightly controlled in the cell. Its activation leads to the generation of metabolizing and scavenging systems to remove excessive ROS, which are detrimental and affect cells functions. Gclm constitutes the rate-limiting enzyme in glutathione synthesis, the most important and most abundant endogenous antioxidant (11). GSH participates in many cellular reactions including antioxidant defenses of the cell, but also cell signaling (11, 15). Indeed, alterations in the redox balance by exposure to ROS cause changes in the reduced/oxidized glutathione (GSH/GSSG) equilibrium, which potentially affect a number of target proteins by causing oxidation at specific cysteine residues, such as the Nrf2 cytoplasmic repressor Keap1 (38). As a consequence, Gclm, as the rate-limiting enzyme in GSH synthesis, could play a crucial role in maintaining an optimal GSH/GSSG balance, providing a protective antioxidant mechanism against oxidative stress-induced cellular dysfunction. On the other hand, contrary to Gclm, the beneficial role of HO-1 and its by-products in atherogenesis has been largely described (7, 29). In vascular cells and macrophages, *HO-1* is induced by most of the well-established cardiovascular risk factors, including oxidized LDLs (43), and Nrf2 is essential for its overexpression (6, 14). The proposed mechanism by which HO-1 exerts its cytoprotective effects includes its ability to degrade pro-oxidative heme, to release biliverdin and subsequently convert it into bilirubin, both of which have antioxidant properties, and to generate carbon monoxide, which has antiproliferative, anti-inflammatory and vasodilatory properties (7, 29). Therefore, HO-1 participates to the anti-atherogenic defence systems of the macrophages, notably by increasing antioxidant protection in atherosclerotic lesions.

Finally, another and very important distinction between OxLDLs and MoxLDLs was observed in the intensity of the induced oxidative stress. As we have shown by the use of Trolox, the oxidized LDL-induced accumulation of ROS is mainly responsible for the activation of Nrf2 and for the overexpression of *Gclm* and *HO-1*, which suggests that the differential oxidative stress generated by OxLDLs and MoxLDLs is the leading cause of the subsequent variations observed in the response to these two types of LDLs. We showed that although NADPH oxidase is implicated in both oxidized LDLs-induced ROS accumulation, the release of AA by some PLA2 isoforms, possibly cPLA2 and/or iPLA2, only takes part in the MoxLDLs-induced activation of NADPH oxidase. This is not surprising since MoxLDLs contrary to OxLDLs, are not affected in their lipid moiety (24, 48), which means that the fatty acids and thus AA, are not modified and can be cleaved by PLA2. This model was supported by the production of MoxLDLs oxidized not only at the protein level, but also at the lipid level, named MoxLDLs-C. Indeed, in specific conditions, MPO can also modify the lipid moiety of the LDL. Fluorescence-based analysis of LDLs showed that the extent of lipid peroxidation in MoxLDLs-C was intermediate between OxLDLs and MoxLDLs. In agreement with our hypothesis, the MoxLDLs-C-induced ROS production was smaller than the one caused by MoxLDLs, but largely higher than the OxLDLs-induced ROS accumulation, indicating that there seems to be an inverse relation between lipid peroxidation in modified LDL and the capacity to induce ROS production. In conclusion, the nonoxidized lipids of LDLs seem to be implicated in the LDLs-induced ROS production. In the presence of NatLDLs, we could hypothesize that their recognition by the LDL-R and not by the scavenger receptors prevents this ROS accumulation, but also that cPLA2 and/or iPLA2, would not be activated (21). This observation underlines an important difference in the ROS-producing mechanisms between OxLDLs and MoxLDLs, which could in part explain the distinct cellular responses observed in this study between both types of LDLs.

In conclusion, this study highlights that at concentrations observed in patients suffering from COPD or in patients under dialysis, the more relevant MoxLDLs that are only modified in their protein moiety, induce a stronger antioxidant and protective response than OxLDLs in macrophages, as revealed by the activation of the Nrf2 pathway. As the oxidative stress plays an important role in the pathogenesis of many diseases, including atherosclerosis, the understanding of redox regulation and the effects of disturbed redox homeostasis on cell functions could be used to develop new strategies for the treatment or prevention of those diseases. In this way, the differential generation of ROS and the distinct ROS-producing mechanisms induced by OxLDLs and MoxLDLs, should be taken into account, and all the data obtained until now with copper oxidized-LDLs carefully re-evaluated taking into consideration physiologically more relevant oxidized LDLs.

ARS-2009-2971-ver9-Calay_1P.3D 06/25/10 11:56pm Page 11

Acknowledgments

This article presents research results of the Belgian Programme on Interuniversity Poles of Attraction (PAI 6/30) initiated by the Belgian State, Prime Minister's Office, Science Policy Programming. Damien Calay and Laurine Mattart are recipients of a doctoral fellowship of the FRIA (Fonds pour la Formation à la Recherche dans l'Industrie et dans l'Agriculture). We also thank the Fonds National de la Recherche Scientifique (FNRS), the Institut de Recherche en Pathologie et Génétique (IRSPG) and the Fonds pour la Recherche Médicale dans le Hainaut for financial support.

Author Disclosure Statement

No competing financial interests exist.

References

1. Akiba S, Yoneda Y, Ohno S, Nemoto M, and Sato T. Oxidized LDL activates phospholipase A2 to supply fatty acids required for cholesterol esterification. *J Lipid Res* 44: 1676–1685, 2003.
2. Alam J and Cook JL. How many transcription factors does it take to turn on the heme oxygenase-1 gene? *Am J Respir Cell Mol Biol* 36: 166–174, 2007.
3. Berliner JA and Heinecke JW. The role of oxidized lipoproteins in atherogenesis. *Free Radic Biol Med* 20: 707–727, 1996.
4. Brennan ML, Anderson MM, Shih DM, Qu XD, Wang X, Mehta AC, Lim LL, Shi W, Hazen SL, Jacob JS, Crowley JR, Heinecke JW, and Lusis AJ. Increased atherosclerosis in myeloperoxidase-deficient mice. *J Clin Invest* 107: 419–430, 2001.
5. Carr AC, Myzak MC, Stocker R, McCall MR, and Frei B. Myeloperoxidase binds to low-density lipoprotein: potential implications for atherosclerosis. *FEBS Lett* 487: 176–180, 2000.
6. Chan K and Kan YW. Nrf2 is essential for protection against acute pulmonary injury in mice. *Proc Natl Acad Sci USA* 96: 12731–12736, 1999.
7. Chung HT, Pae HO, and Cha YN. Role of heme oxygenase-1 in vascular disease. *Curr Pharm Des* 14: 422–428, 2008.
8. Daugherty A, Dunn JL, Rateri DL, and Heinecke JW. Myeloperoxidase, a catalyst for lipoprotein oxidation, is expressed in human atherosclerotic lesions. *J Clin Invest* 94: 437–444, 1994.
9. Deng TL, Yu L, Ge YK, Zhang L, and Zheng XX. Intracellular-free calcium dynamics and F-actin alteration in the formation of macrophage foam cells. *Biochem Biophys Res Commun* 338: 748–756, 2005.
10. Droge W. Free radicals in the physiological control of cell function. *Physiol Rev* 82: 47–95, 2002.
11. Franco R, Schoneveld OJ, Pappa A, and Panayiotidis MI. The central role of glutathione in the pathophysiology of human diseases. *Arch Physiol Biochem* 113: 234–258, 2007.
12. Hazen SL and Heinecke JW. 3-Chlorotyrosine, a specific marker of myeloperoxidase-catalyzed oxidation, is markedly elevated in low density lipoprotein isolated from human atherosclerotic intima. *J Clin Invest* 99: 2075–2081, 1997.
13. Hwang J, Ing MH, Salazar A, Lassegue B, Griendling K, Navab M, Sevanian A, and Hsiai TK. Pulsatile versus oscillatory shear stress regulates NADPH oxidase subunit expression: Implication for native LDL oxidation. *Circ Res* 93: 1225–1232, 2003.
14. Ishii T, Itoh K, Ruiz E, Leake DS, Unoki H, Yamamoto M, and Mann GE. Role of Nrf2 in the regulation of CD36 and stress protein expression in murine macrophages: activation by oxidatively modified LDL and 4-hydroxynonenal. *Circ Res* 94: 609–616, 2004.
15. Jefferies H, Coster J, Khalil A, Bot J, McCauley RD, and Hall JC. Glutathione. *ANZ J Surg* 73: 517–522, 2003.
16. Kensler TW, Wakabayashi N, and Biswal S. Cell survival responses to environmental stresses via the Keap1-Nrf2-ARE pathway. *Annu Rev Pharmacol Toxicol* 47: 89–116, 2007.
17. Kim C, Kim JY, and Kim JH. Cytosolic phospholipase A(2), lipoxygenase metabolites, and reactive oxygen species. *BMB Rep* 41: 555–559, 2008.
18. Klinkner AM, Waites CR, Kerns WD, and Bugelski PJ. Evidence of foam cell and cholesterol crystal formation in macrophages incubated with oxidized LDL by fluorescence and electron microscopy. *J Histochem Cytochem* 43: 1071–1078, 1995.
19. Lee JM and Johnson JA. An important role of Nrf2-ARE pathway in the cellular defense mechanism. *J Biochem Mol Biol* 37: 139–143, 2004.
20. Leeuwenburgh C, Rasmussen JE, Hsu FF, Mueller DM, Pennathur S, and Heinecke JW. Mass spectrometric quantification of markers for protein oxidation by tyrosyl radical, copper, and hydroxyl radical in low density lipoprotein isolated from human atherosclerotic plaques. *J Biol Chem* 272: 3520–3526, 1997.
21. Lupo G, Nicotra A, Giurdanella G, Anfuso CD, Romeo L, Biondi G, Tirolo C, Marchetti B, Ragusa N, and Alberghina M. Activation of phospholipase A(2) and MAP kinases by oxidized low-density lipoproteins in immortalized GP8.39 endothelial cells. *Biochim Biophys Acta* 1735: 135–150, 2005.
22. Lusis AJ. Atherosclerosis. *Nature* 407: 233–241, 2000.
23. Maines MD. The heme oxygenase system: A regulator of second messenger gases. *Annu Rev Pharmacol Toxicol* 37: 517–554, 1997.
24. Malle E, Marsche G, Arnhold J, and Davies MJ. Modification of low-density lipoprotein by myeloperoxidase-derived oxidants and reagent hypochlorous acid. *Biochim Biophys Acta* 1761: 392–415, 2006.
25. Marsche G, Zimmermann R, Horiuchi S, Tandon NN, Sattler W, and Malle E. Class B scavenger receptors CD36 and SR-BI are receptors for hypochlorite-modified low density lipoprotein. *J Biol Chem* 278: 47562–47570, 2003.
26. Maziere C and Maziere JC. Activation of transcription factors and gene expression by oxidized low-density lipoprotein. *Free Radic Biol Med* 2008.
27. McMillen TS, Heinecke JW, and LeBoeuf RC. Expression of human myeloperoxidase by macrophages promotes atherosclerosis in mice. *Circulation* 111: 2798–2804, 2005.
28. Moguilevsky N, Zouaoui Boudjeltia K, Babar S, Delree P, Legssyer I, Carpentier Y, Vanhaeverbeek M, and Ducobu J. Monoclonal antibodies against LDL progressively oxidized by myeloperoxidase react with ApoB-100 protein moiety and human atherosclerotic lesions. *Biochem Biophys Res Commun* 323: 1223–1228, 2004.
29. Morita T. Heme oxygenase and atherosclerosis. *Arterioscler Thromb Vasc Biol* 25: 1786–1795, 2005.
30. Morse D and Choi AM. Heme oxygenase-1: The "emerging molecule" has arrived. *Am J Respir Cell Mol Biol* 27: 8–16, 2002.
31. Muller K, Dulku S, Hardwick SJ, Skepper JN, and Mitchinson MJ. Changes in vimentin in human macrophages during apoptosis induced by oxidised low density lipoprotein. *Atherosclerosis* 156: 133–144, 2001.
32. Nicholls SJ and Hazen SL. Myeloperoxidase and cardiovascular disease. *Arterioscler Thromb Vasc Biol* 25: 1102–1111, 2005.

ARS-2009-2971-ver9-Calay_1P.3D 06/25/10 11:56pm Page 12

33. Sharif O, Bolshakov VN, Raines S, Newham P, and Perkins ND. Transcriptional profiling of the LPS induced NF-kappaB response in macrophages. *BMC Immunol* 8: 1, 2007.
34. Shiose A and Sumimoto H. Arachidonic acid and phosphorylation synergistically induce a conformational change of p47phox to activate the phagocyte NADPH oxidase. *J Biol Chem* 275: 13793–13801, 2000.
35. Singh U and Jialal I. Oxidative stress and atherosclerosis. *Pathophysiology* 13: 129–142, 2006.
36. Stocker R and Keaney JF, Jr. Role of oxidative modifications in atherosclerosis. *Physiol Rev* 84: 1381–1478, 2004.
37. Thomas CE. The influence of medium components on Cu(2+)-dependent oxidation of low-density lipoproteins and its sensitivity to superoxide dismutase. *Biochim Biophys Acta* 1128: 50–57, 1992.
38. Townsend DM, Tew KD, and Tapiero H. The importance of glutathione in human disease. *Biomed Pharmacother* 57: 145–155, 2003.
39. Vaes M, Zouaoui Boudjeltia K, Van Antwerpen P, Babar S, Deger F, Vanhaeverbeek M, and Ducobu J. Low-density lipoprotein oxidation by myeloperoxidase occurs in the blood circulation during hemodialysis. *Atherosclerosis Supplements* 7: 525, 2006.
40. Valko M, Leibfritz D, Moncol J, Cronin MT, Mazur M, and Telser J. Free radicals and antioxidants in normal physiological functions and human disease. *Int J Biochem Cell Biol* 39: 44–84, 2007.
41. Wittwer J and Hersberger M. The two faces of the 15-lipoxygenase in atherosclerosis. *Prostaglandins Leukot Essent Fatty Acids* 77: 67–77, 2007.
42. Yagi K. A simple fluorometric assay for lipoperoxide in blood plasma. *Biochem Med* 15: 212–216, 1976.
43. Yamaguchi M, Sato H, and Bannai S. Induction of stress proteins in mouse peritoneal macrophages by oxidized low-density lipoprotein. *Biochem Biophys Res Commun* 193: 1198–1201, 1993.
44. Yan LJ, Lodge JK, Traber MG, Matsugo S, and Packer L. Comparison between copper-mediated and hypochlorite-mediated modifications of human low density lipoproteins evaluated by protein carbonyl formation. *J Lipid Res* 38: 992–1001, 1997.
45. Yokoyama C, Wang X, Briggs MR, Admon A, Wu J, Hua X, Goldstein JL, and Brown MS. SREBP-1, a basic-helix-loop-helix-leucine zipper protein that controls transcription of the low density lipoprotein receptor gene. *Cell* 75: 187–197, 1993.
46. Zarev S, Bonnefont–Rousselot D, Jedidi I, Cosson C, Couturier M, Legrand A, Beaudeux JL, and Therond P. Extent of copper LDL oxidation depends on oxidation time and copper/LDL ratio: chemical characterization. *Arch Biochem Biophys* 420: 68–78, 2003.
47. Ziouzenkova O, Sevanian A, Abuja PM, Ramos P, and Esterbauer H. Copper can promote oxidation of LDL by markedly different mechanisms. *Free Radic Biol Med* 24: 607–623, 1998.
48. Zouaoui Boudjeltia K, Legssyer I, Van Antwerpen P, Kisoka RL, Babar S, Moguilevsky N, Delree P, Ducobu J, Remacle C, Vanhaeverbeek M, and Brohee D. Triggering of inflammatory response by myeloperoxidase-oxidized LDL. *Biochem Cell Biol* 84: 805–812, 2006.
49. Zouaoui Boudjeltia K, Tragas G, Babar S, Moscariello A, Nuyens V, Van Antwerpen P, Gilbert O, Ducobu J, Brohee D, Vanhaeverbeek M, and Van Meerhaeghe A. Effects of oxygen therapy on systemic inflammation and myeloperoxidase modified LDL in hypoxemic COPD patients. *Atherosclerosis* 2009.

Address correspondence to:
Damien Calay
University of Namur (FUNDP)—URBC
Rue de Bruxelles 61
5000 Namur
Belgium

E-mail: damien.calay@fundp.ac.be

Date of first submission to ARS Central, October 27, 2009; date of final revised submission, April 27, 2010; date of acceptance, May 1, 2010.

Abbreviations Used

AA = arachidonic acid
ARE = antioxidant response element
COPD = chronic obstructive pulmonary disease
cPLA2 = calcium-dependent cytosolic phospholipase A2
DPI = diphenylene iodonium chloride
Gclm = glutamate cysteine ligase, regulatory subunit
GSH = reduced glutathione
GSSG = oxidized glutathione
H_2DCF-DA = 2′,7′-dichlorodihydrofluorescein diacetate
HO-1 = heme oxygenase-1
iPLA2 = calcium-independent cytosolic phospholipase A2
LDLs = low-density lipoproteins
LDL-R = LDL receptor
MAFP = methyl arachidonyl fluorophosphonate
M-CSF = macrophage colony stimulating factor
MoxLDLs = myeloperoxidase-oxidized LDLs
rhMPO = recombinant human myeloperoxidase
NatLDLs = native LDLs
Nrf2 = NF-E2-related factor 2
OxLDLs = copper-oxidized LDLs
PBMC = peripheral blood mononuclear cells
ROS = reactive oxygen species
Trolox = 6-hydroxy-2,5,7,8-tetramethylchromane-2-carboxylic acid

Supplemental data: Calay *et al.* ARS.2009.2971

www.liebertonline.com/ars

Supplemental Materials and Methods

Reagents and antibodies

All reagents were obtained from Merck Biosciences (Nottingham, UK) unless otherwise specified. Trolox (6-hydroxy-2,5,7,8-tetramethylchromane-2-carboxylic acid) and Oil Red O were obtained from Sigma-Aldrich (St. Louis, MO). The fluorescent dyes H_2DCF-DA and Bodipy® were purchased from Invitrogen (Carlsbad, CA). CHO-expressed recombinant human M-CSF was from R&D Systems (Abingdon, UK). The Gclm antibody was purchased from Santa Cruz Biotechnologies (Santa Cruz, CA), the HO-1 antibody from Abcam (Cambridge, UK), the ERK2 antibody was obtained from BD Biosciences (San Jose, CA) and the secondary HRP- or Alexa-conjugated antibodies were from Amersham Biosciences and Molecular Probes, Invitrogen (Carlsbad, CA), respectively.

Oil Red O staining

RAW 264.7 macrophages were seeded in 12-well plates (45,000 cells/cm^2). After incubation with LDLs, the cells were rinsed twice with PBS, and then fixed with paraformaldehyde 4% for 2.5 min. Three volumes of Oil Red O (0.2 % in isopropanol) mixed with two volumes of dextrine (1% in distilled water) were filtered through a Whatman filter and put on the cells for 30 min. After three rinses with PBS, the lipid staining by Oil Red O was visualized with an optical microscope (Leica; Objective 20X). The staining was then quantified by measuring the absorbance at 490 nm after solubilization in ethanol for 30 min. These values were normalized by the quantity of cells, evaluated by propidium iodide (10 μg/ml for 30 min; $\lambda_{exc.} = 515$ nm, $\lambda_{em.} = 612$ nm).

Measurement of reactive oxygen species production

RAW 264.7 cells were seeded in 24-well plates (100,000 cells/cm^2) and left to adhere overnight. The cells were incubated with 20 μM dichloro-dihydro-fluorescein diacetate (H_2DCF-DA) for 30 min at 37°C in the dark, washed twice with PBS, and then treated with native or oxidized LDLs (200 μg/ml). After various incubation times at 37°C in the dark, the intracellular oxidation of H_2DCF by ROS was quantified by measurement of DCF fluorescence at 520 nm ($\lambda_{exc.} = 485$ nm) with a Fluoroskan Ascent fluorimeter (Thermo Scientific, Waltham, MA). The protein concentration was measured by the Bradford method after lysis in 1 *N* NaOH and the fluorescence was expressed as relative fluorescence in AU per mg protein for normalization.

Transfection experiments

RAW 264.7 macrophages were transfected with the ARE-luciferase reporter plasmid containing the luciferase coding sequence driven by the authentic promoter of *NQO1* bearing one ARE sequence (ARE-luc). Briefly, the day before transfection, the cells were plated at 52,000 cells/cm^2 in 12-well plates. The day after, complexes made of 1 μg of ARE-luc mixed with 2 μl of Lipofectamine 2000 (Invitrogen) diluted in OptiMEM (Gibco BRL, Invitrogen), were added to the cells and left overnight. Cells were rinsed and then treated with NatLDLs, OxLDLs, or MoxLDLs for an additional period of 24 h before lysis with Glo lysis buffer (Promega, Madison, WI). The cell lysate was mixed in an equal volume with the Bright Glo luciferase substrate (Promega) and the luminescence was directly measured with a Luminoskan Ascent luminometer (Thermo Scientific). Total protein was measured by the Bradford assay and used to normalize the luminescence in RLU per mg protein.

siRNA transfection

RAW 264.7 cells were transfected three times every 24 h with 10 n*M* anti-Nrf2 siRNA (SMARTpool® siRNA, Upstate/Dharmacon, Lafayette, CO) or 10 n*M* nontargeting (NT) siRNA (Upstate/Dharmacon) using Interferin (Polyplus, Lucron Bioproducts, De Pinte, Belgium) as transfection reagent, following the manufacturer's instructions. Briefly, siRNA was diluted in OptiMEM, mixed with Interferin and incubated 10 min at room temperature. RAW 264.7 at approximatively 50% of confluence were incubated in DHG-L1 without serum and siRNA/Interferin complexes were added on the cells for 24 h. The next 2 days, the cells were rinsed with DHG-L1 without serum in order to remove all complexes and incubated with siRNA/Interferin complexes again, as mentioned above. Twenty-four h after the third and last transfection, the cells were rinsed with DHG-L1 without serum and placed in DHG-L1 containing 1% of heat-inactivated serum before stimulation with NatLDLs, OxLDLs, or MoxLDLs.

Total RNA extraction, reverse transcription, and real-time RT-PCR analysis

Total RNA was extracted from stimulated cells using the RNAgents kit from Promega (Madison, WI) following the manufacturer's procedure. After quantification, 5 μg of total RNA were used for the reverse transcription reaction. Briefly, total RNA was incubated with 1 μg of oligo dT (Invitrogen) for 10 min at 70°C, then 0.1 *M* DTT (Invitrogen), RNAsin (40 U/μl) (Invitrogen), dNTP mix (Eurogentec, Belgium), and Superscript RII reverse transcriptase (200 U/μl) (Invitrogen) were added. The reverse transcription reaction was performed for 90 min at 42°C. cDNA was obtained after incubation with RNase H (2U/μl) (Invitrogen) for 20 min at 37°C. 12.5 μl of SYBRGreen PCR Master Mix (Applied Biosystems, Warrington, UK), 2.5 μl of 300 n*M* forward (5′ TCCACAGCCCGACAGCAT 3′) and 300 n*M* reverse (5′ ATTCTC GGCTTGGATGTGTACCT 3′) murine *HO-1* primers; 300 n*M* forward (5′ GCAGTCAGGCAGAGGGTGATA 3′) and 300 n*M* reverse (5′ CAACTCCTCAAAGAGCTGGATGTT 3′) human *HO-1* primers ; 300 n*M* forward (5′ CAGTTACAG GTGGCAGCATGA 3′) and 300 n*M* reverse (5′ TAGTGCTG CAGGGTGATTTCAG 3′) murine *TBP* primers; 300 n*M* forward (5′ TGGTGCATGGCCGTTCT 3′) and 300 n*M* reverse (5′ TAGTTAGCATGCCAGAGTCTCGTT 3′) human *18S* primers; 900 n*M* forward (5′ TTGACATACAGCTACTGAC TCACAATG 3′) and 900 n*M* reverse (5′ CAATGTCAGG GATGCTTTCTTG 3′) murine *Gclm* primers in 20 μl final volume, were mixed with 5 μl of 100 times diluted cDNA. Real-time RT-PCR was performed with the Abi-Prism 7000

Sequence Detection System (Applied Biosystems) and data were subjected to relative quantification using *TBP* as endogenous reference for normalization. The ∂∂Ct method was applied to each sample in order to calculate the relative fold induction.

Immunoblotting analysis

After treatment, the cells were washed with ice-cold PBS and scraped in 100 μl of Lysis buffer (10 m*M* Tris-HCl pH 7.4, 100 m*M* NaCl, 10% glycerol, 1% NP-40, 0.1% SDS, 0.5% sodium deoxycholate, protease inhibitor cocktail (Roche), 1 μM $NaVO_3$, 10 μM PNPP, 10 μM β-glycero-phosphate, 5 μM NaF). After incubation on ice for 30 min, the lysates were centrifuged 10 min at 13,000 rpm (4°C) (5415R centrifuge (Eppendorf, Hamburg, Germany)) and the supernatants were collected. Protein concentration was evaluated by the Bradford method. 30 μg of proteins were separated in 12% SDS-PAGE gels, blotted onto a polyvinylidene difluoride membrane (Amersham Biosciences, Pittsburgh, PA) for 2 h at 150 mA. After blocking for 2 h in TBS containing 0.1 % Tween 20 (Sigma-Aldrich, St. Louis, MO) (TBS-T) and 2% Amersham blocking reagent (Amersham Biosciences), the membrane was incubated with the primary antibody diluted in TBS-T containing 2% of Amersham blocking reagent overnight at 4°C. The membrane was washed three times for 15 min with TBS-T, incubated 45 min at room temperature with specific secondary antibodies coupled to HRP, and washed again three times for 15 min with TBS-T before protein detection using the ECL system (Amersham Biosciences).

Immunofluorescence and labelling of lipid droplets by Bodipy®

RAW 264.7 cells, plated on glass coverslips in 24-well plates, were washed twice with PBS, fixed with 4% paraformaldehyde for 10 min and permeabilized in PBS containing 1% Triton X-100 for 5 min. After blocking with PBS containing 2% bovine serum albumin, the cells were incubated overnight at 4°C with the diluted primary antibody followed, after washing, by the incubation with the Alexa Fluor® 488 goat anti-rabbit IgG antibody for 1 h in the dark at room temperature. For the Bodipy staining, after blocking, the cells were incubated for 1 h with the Bodipy dye (20 μg/ml) at room temperature. Nuclei were stained by Topro3 for 35 min in the dark at room temperature. After washing with PBS, coverslips were mounted with Mowiol and the samples were examined by confocal fluorescence microscopy (Leica TCS SP2) equipped with a Zeiss oil immersion 63X objective.

Measurement of lipid peroxidation

Lipid peroxidation was measured according to the technique proposed by Yagi *et al.* (1), by adding 4.0 ml of sulfuric acid (N/12) and 500 μl of phosphotungstic acid (10%) to 200 μl of LDL solution. After 5 min, the tubes were centrifuged at 1600 *g* for 10 min, and the supernatant discarded. The residue was suspended in sulfuric acid (2.0 ml) and phosphotungstic acid (300 μl) for 10 min. The tubes were centrifuged at 1600 *g* for 10 min and the supernatant discarded again. The residue was dissolved in 4.0 ml of water and 1.0 ml of a thiobarbituric acid reagent in acetic acid (335 mg in 50.0 ml of water diluted 50:50 in acetic acid 99%). The tubes were incubated 1 h at 95°C. The solutions were cooled and the product of the reaction was extracted by 5.0 ml of n-butanol. The fluorescence of the organic layer was measured at 553 nm with an excitation at 515 nm. The concentration of the total lipid peroxide (expressed in nmol per mg of LDL) was calculated with the slope obtained from a gradient concentration of tetramethoxypropane pure standard diluted in 4.0 ml of water and 1.0 ml of the thiobarbituric acid reagent.

Reference

1. Yagi K. A simple fluorometric assay for lipoperoxide in blood plasma. *Biochem Med* 15: 212–216, 1976.

AUTHOR QUERY FOR ARS-2009-2971-VER9-CALAY_1P

AU1: Use of word «obtention» not clear. Please provide another word.
AU2: '§§§' symbol not found in the figure. Please check.
AU3: Part label 'B' is not found in the figure 2 legend. Please check.
AU4: Part labels 'A' & 'B' is not found in the figure 5 legend. Please check.
AU5: Part label 'C' is not found in the figure 7 legend. Please check.